Microscopic analysis of voltage noise operation mode in SiGe/Si bipolar heterojunctions: Influence of the SiGe strained layer

M. J. Martín,[a] D. Pardo, and J. E. Velázquez
Dpto. de Física Aplicada, Universidad de Salamanca, Pza. De la Merced s/n, 37008 Salamanca, Spain

(Received 14 January 2000; accepted for publication 18 April 2000)

A Monte Carlo analysis of bipolar transport and voltage fluctuations in a p^+-Si/n-$Si_{0.7}Ge_{0.3}$ heterojunction and in a p^+n Si homojunction under different operation regimes is presented. Comparison of the spectral density of voltage fluctuations at low frequency, $S_V(x,0)$, between both structures reveals the strong effect of the SiGe layer on the noise behavior in the heterojunction. Alloy scattering hinders the electron mobility enhancement expected from the removal of valley degeneracy in the SiGe layer. Despite this mobility reduction, the greater accumulation of carriers in the low-doped region supported by the valence band discontinuity reduce $S_V(x,0)$ in the heterojunction for a given average voltage. This study also reveals the impact of hot carriers on noise performance in the quasisaturation regime of both diodes. © *2000 American Institute of Physics.* [S0021-8979(00)02215-5]

I. INTRODUCTION

Si-compatible heterostructure devices, based on epitaxial growth of $Si_{1-x}Ge_x$ strained layers on relaxed Si, have recently aroused strong interest as regards the design of high-speed circuits. In particular, the incorporation of Ge in the base of silicon bipolar transistors allows dramatic improvements in the speed and noise performance of bipolar circuits together with a modest increase in the complexity of technological processes.[1,2] In the development of these new $Si_{1x}Ge_x$/Si technologies for high-frequency applications a key factor is a physically based characterization of the electronic noise properties of the $Si_{1-x}Ge_x$/Si heterojunction. This emphasizes the importance of a better understanding of the relationship between microscopic transport phenomena and the mechanisms governing noise in heterojunction bipolar devices. Currently, the ensemble Monte Carlo method (EMC) is the most rigorous approach for the study of the nonstationary carrier transport in submicron devices.[3] Additionally, this method allows one to gain a microscopic understanding of the different noise sources because these are intrinsically included in the microscopic transport model. The EMC method has been successfully employed to investigate the current and voltage fluctuations in different high-speed unipolar devices: n^+nn^+ junctions, Schottky diodes, and GaAs metal semiconductor field effect transistor.[4–6]

This article addresses the influence on noise of a $Si_{1-x}Ge_x$ strained layer on voltage fluctuations in a n-SiGe/p^+-Si diode as a first step in the study of noise in more complex heterostructures. The method used in the voltage noise operation mode has been described previously for unipolar[7] as well as p^+n and pn^+ Si homojunctions.[8] It provides a spatial analysis of the spectral density of voltage fluctuations under constant-current conditions and therefore affords the exact positions of the different noise sources inside the device. The method is based on the following: For a structure of length L in the simulated direction, the total current through the structure is maintained constant over time: $I(t)=I_o$. Accordingly, the relationship which, at each time step, gives the deviation of voltage drop between terminals, $\Delta V(L,t)=V(L,t)-V(0,t)$, with respect to an average applied voltage, V_{aver}, can be written as

$$\frac{d}{dt}\Delta V(L,t)=\frac{L}{A\epsilon_r\epsilon_o}[I_c(t)-I_o], \tag{1}$$

where ϵ_o is the free-space permitivity; ϵ_r is the relative static dielectric constant of the material; A is the cross-sectional area, and $I_c(t)$ is the instantaneous value of the conduction current inside the device.[8]

Through the resolution, at each time step, of the Poisson equation, this procedure allows one to calculate the instantaneous voltage fluctuations along the device: $\delta V(0\leqslant x\leqslant L, t=n\Delta t)$. This method was made suitable for the resolution of the iterative algorithm in which Eq. (1) is solved with the appropriate boundary conditions at both sides of the heterojunctions by taking into account the different values of the dielectric constant in the Si and in the SiGe layers.

II. SIMULATED STRUCTURES AND AVERAGE MAGNITUDES OF INTEREST

Our study was conducted in two diodes: a Si p^+n homojunction ($H1$) and a p^+-Si/n-$Si_{0.7}Ge_{0.3}$ heterojunction ($H2$). The doping profile was considered to be abrupt and with the same level in both diodes. Impurity concentrations were 10^{17} and $5\times10^{15}\,\text{cm}^{-3}$ in the p^+ and the n regions, respectively. The band structure and the scattering mechanisms involved in the electron and hole transport in Si and strained SiGe implemented in our EMC simulator have been previously explained in detail in Refs. 9–11. The growing of SiGe alloy on [001] Si splits the X valleys into: (a) shifted down valleys ([100] and [010]) designated here as $X_\perp$ and (b) [001] valleys or $X_\parallel$ (Fig. 1). Regarding the valence band (VB), one of the most important effects in the pseudomor-

[a]Electronic mail: mjesus@rs6000.usal.es

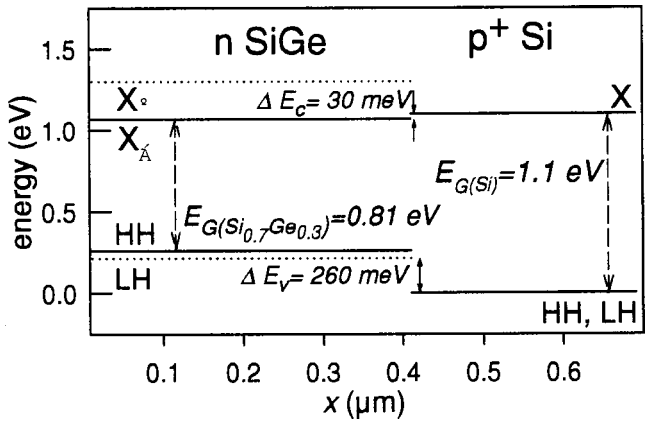

FIG. 1. Scheme of the band alignment of the p^+-Si/n-$Si_{0.7}Ge_{0.3}$ structure with its characteristic parameters, the valence and conduction band offsets, and geometry.

phic $Si_{1-x}Ge_x$ layers is the reduction in the gap, mainly originated by an upward shift of the nondegenerated heavy-hole (HH) and light-hole (LH) subbands.[11] In our calculations we assumed that the SiGe layer was fully strained (in spite of the fact that its thickness was larger than the critical one[12]) in order to facilitate comparison of the results for $H1$ and $H2$. Neither surface and bulk generation-recombination processes nor quantum corrections to the total current were considered in the model.

Figure 2 shows the electron and hole current densities versus the average applied voltage ($J_e, J_h - V_{aver}$) of both structures. In the case of $H1$, for $V_{aver} < V_{bi}$ (0.73 V), J_e and J_h, exhibit an exponential dependence on V_{aver} typical of barrier-controlled transport in *low injection conditions*.[13] For $V_{aver} > V_{bi}$, both quantities tend to exhibit a more ''linear'' dependence. For $V_{aver} > 0.80$ V the structure enters in *high injection conditions*. In view of the J_e, $J_h - V_{aver}$ characteristics of $H2$, certain differences should be highlighted with respect to those of $H1$. First, the J_h/J_e ratio is larger than in the homojunction case due to the strong increase in J_h, reflecting the existence of the VB discontinuity at the heterojunction. Second, the character of the $J_h - V_{aver}$ characteristics is modified in $H2$. For $V_{aver} < V_{bi}$, the slope of $J_h - V_{aver}$ differs from the typical one of the *low-injection regime*, while J_e continues to show a similar behavior to that seen in $H1$.

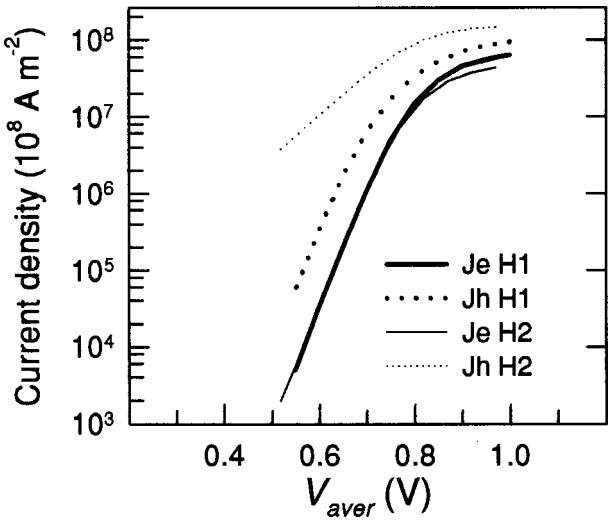

FIG. 2. Electron and hole current density-average applied voltage characteristics of $H1$ and $H2$.

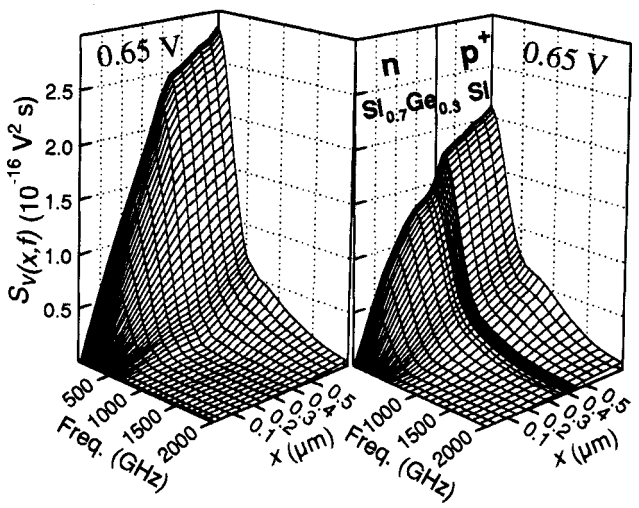

FIG. 3. $S_V(x,f)$ vs frequency, f, and position, x, in $H1$ (left plot) and $H2$ (right plot) for an average voltage of 0.65 V.

III. SPATIAL STUDY OF VOLTAGE FLUCTUATIONS

Figure 3 shows the spectral density of the voltage fluctuations, $S_V(x,f)$, across both structures (we took the voltage reference at the ohmic contact in the n-type region) for $V_{aver} = 0.65$ V. The total current density through the structure, I_o/A, is equal to 1.86×10^6 A m^{-2} in $H1$ and 2.07×10^7 A m^{-2} in $H2$. In the light of this figure, two different behaviors can be distinguished for high and for low frequencies. At very high frequencies (around 1000 GHz) it can be seen that the value of $S_V(L,f)$ is determined by spatial growth of $S_V(x,f)$ in the highly doped regions of $H1$ and $H2$. This growth takes place at frequencies related to the plasma frequency of the holes (majority carriers of the p^+ Si region), indicating that the plasma oscillations dominate the voltage fluctuations.[4] This well localized growth is partially masked by contributions to noise arising from lower frequencies.

The low-frequency values of the spectral density of voltage fluctuations, $S_V(x,0)$, are strongly related to the internal mechanisms that control noise in the device (band discontinuities, alteration of transport properties of the SiGe layer due to strain, the presence of hot carriers). In Fig. 4 we show $S_V(x,0)$ for both structures and several values of the average voltage. A detailed analysis of $S_V(x,0)$ in the homojunction has been previously reported,[8] and hence here we focused on the differences in $S_V(x,0)$ of $H2$ with respect to $H1$.

To analyze these results, we first observe the contribution to $S_V(x,0)$ of the layer common to both structures: the Si p^+ region. In the neutral region of the p^+ side of $H1$ and $H2$, the values obtained for $S_V(x,0)$ are in agreement with those obtained using a single resistance in the Nyquist theorem:[7] $S_V(x,0)$ exhibits a slight linear dependence on the

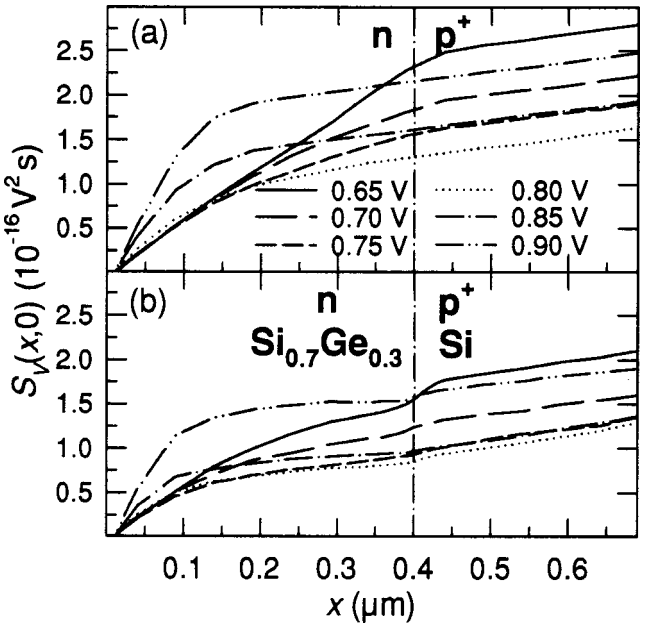

FIG. 4. $S_V(x,0)$ as a function of the position in $H1$ (upper plot) and $H2$ (lower plot) for different average voltages. The line types and applied voltages are valid for both plots.

position (due to the low resistivity of the region) and is essentially determined by the quasiconstant hole concentration [Fig. 5(a)] Accordingly, no significant differences in the slope of $S_V(x,0)$ in the Si region between both diodes are found and therefore the differences in $S_V(x,0)$ between both structures must arise from the n regions.

Let us analyze separately the contributions to voltage noise in all the well-defined operation regimes in $H1$ and $H2$. In the *low injection regime* [0.65 V in $H1$, Fig. 4(a)] $S_V(x,0)$ is generated in the low doping region (n region) due to its high resistance. The negligible concentration of holes in the neutral n region makes the majority carriers determine the resistance and hence, along the structure, $S_V(x,0)$ exhibits a linear dependence on the position with two different slopes in the neutral p^+ and in the n regions (in agreement with the Nyquist theorem).

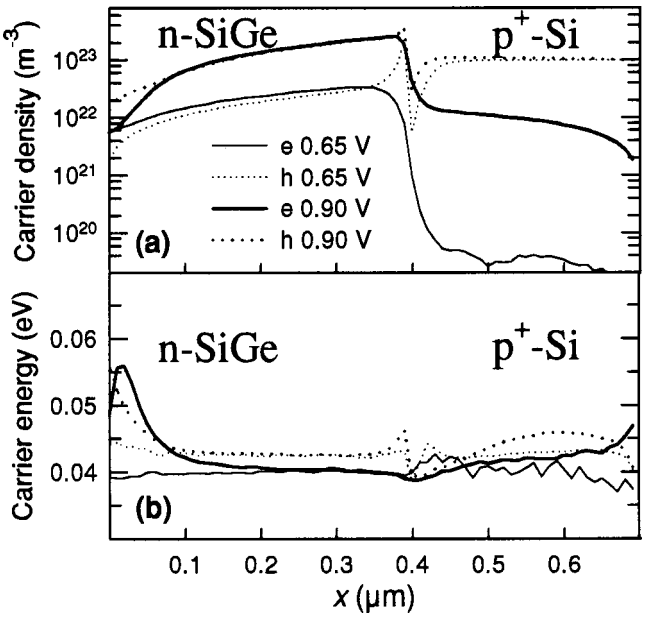

FIG. 5. Comparison of electron and hole concentrations (a) and electron and hole mean energy (b) as a function of position through $H2$ for 0.65 (hairline) and 0.85 V (thicker line).

When the diodes leave the low injection regime, $S_V(x,0)$ is strongly modified across the n region and, for the same value of V_{aver}, the heterojunction exhibits lower values of $S_V(L,0)$. Let us attempt to clarify the origin of this behavior. In the low-doped $Si_{0.7}Ge_{0.3}$ strained layer under consideration, the strong alloy scattering hinders the electron mobility enhancement expected from the removal of valley degeneracy and the reduced effective mass of the electrons (essentially that of the $X_{\|}$ valleys).[14–16] Therefore, this mobility reduction opposes the decrease of $S_V(x=L,0)$ in $H2$ with respect to $H1$. Thus, all the advantages gained by reducing the SiGe layer resistance that we might have expected on the basis of degeneracy lifting are cancelled by this strong scattering. However, this decrease in $S_V(x,0)$ in $H2$ can be explained by the influence of the band discontinuity on the transport in $H2$ and will be analyzed in detail. First, the kinetic energy of a hole crossing the heterojunction towards the n region increases by 260 meV due to the valence-band discontinuity (ΔE_v). Since holes gain a high value of kinetic energy in this process their scattering probability also rises strongly and this determines a fast relaxation of this energy. This leads to a noticeable maximum in the profile of the average kinetic energy located at 0.39 μm from the n-side contact in Fig. 5(b) (since we plot the average kinetic energy of the particles in each mesh cell, not only the energy of the particles crossing the heterojunction, the value of the maximum is substantially lower than ΔE_v).

Second, the VB discontinuity also establishes a spike in the concentration of holes [Fig. 5(a)]: this is the origin of a strong accumulation of electrons and holes in the SiGe layer. Even for the lowest V_{aver} considered (0.65 V) the SiGe region operates under high-injection conditions. As V_{aver} increases, carrier accumulation is enhanced in the n region, determining both a slope of the J_h different from that found in $H1$[13] and a nonconstant slope of $S_V(x,0)$ in the whole SiGe region [Fig. 4(b)]. For $V_{\text{aver}}>0.80$ V the n region of $H1$ also enters the high-injection regime and, as V_{aver} increases for both diodes, $S_V(L,0)$ is strongly lowered. For a given V_{aver} this reduction remains more pronounced in $H2$ owing to the lower resistivity of this diode which, despite the carrier mobility degradation in the SiGe layer, is related to the strong carrier accumulation supported by the VB discontinuity.

For the largest V_{aver} studied (0.85 and 0.90 V), both diodes are in the quasisaturated region and the shape of $S_V(x,0)$ becomes almost identical in both diodes [Figs. 4(a) and 4(b)]. When the structures enter the high-injection regime there is an important accumulation of minority carriers across the low-doped regions, and the depletion region disappears. We employed state of the art boundary conditions[10,17,18] for modeling the ohmic contacts which dynamically maintain the majority carrier concentration equal to the impurity density in a region close to the contact. Be-

cause in the modeling of ohmic boundary conditions excess free-carrier charge is not removed by the algorithm[18] in a zone close to the ohmic contact[10] at $x=0\ \mu$m, an electric field is self-established which forces the minority carriers (holes) to leave the structure. As a consequence of this, in the aforementioned zone close to the terminal in the weakly doped regions, a strong reduction in conductivity appears, leading to a rise in $S_V(x,0)$ in both the homojunction and the heterojunction.

In addition to the above-discussed factors, it is possible to appreciate an increase in $S_V(x,0)$ in a thin zone located at both sides of the heterojunction that is different in slope from that found in $H1$. This difference arises from the band discontinuity and, locally, increases the contributions to noise in $H2$.

IV. CONCLUSIONS

A one-dimensional Monte Carlo study of voltage noise fluctuations in a p^+-Si/n-$Si_{0.7}Ge_{0.3}$ abrupt heterojunction and a p^+n Si homojunction was performed. This study was comparative in nature and focused on the differences in $S_V(x,f)$ between both structures yielded by the presence of the SiGe layer. According to the origin of the high frequency voltage fluctuations (plasma oscillations of majority carriers of the p^+ Si region), we found similar behavior in the homostructure and the heterostructure.

Regarding low-frequency performance, $S_V(x,0)$ is strongly related to the internal mechanisms that control noise in the device. In the p^+-Si region no difference in $S_V(x,0)$ is found between either diode. As V_{aver} increases, $S_V(x,0)$ is strongly modified across the n region and, for the same value of V_{aver}, the heterojunction exhibits lower values of $S_V(L,0)$. The $S_V(x=L,0)$ behavior is strongly controlled by the influence of the band discontinuity in the transport in heterojunction. For a given V_{aver}, the $S_V(x=L,0)$ reduction remains more pronounced in the heterojunction owing to the lower resistivity of this diode which, despite degradation of the carrier mobility in the SiGe layer, is related to the strong carrier accumulation supported by the VB discontinuity.

ACKNOWLEDGMENTS

This work has been funded by Research Project PB97-1331 from the Dirección General de Enseñanza Superior e Investigación Científica and Research Project SA44/99 from the Junta de Castilla y León.

[1] J. D. Cressler, IEEE Trans. Microwave Theory Tech. **46**, 572 (1998).
[2] D. L. Harame, J. H. Comfort, J. D. Cressler, E. F. Crabbé, J. Y.-C. Sun, B. S. Meyerson, and T. Tice, IEEE Trans. Electron Devices **42**, 469 (1995).
[3] C. Jacoboni and P. Lugli, *The Monte Carlo Method for Semiconductor Device Simulation* (Spinger, Vienna, 1989).
[4] J. Zimmermann and E. Constant, Solid-State Electron. **23**, 915 (1980).
[5] L. Varani, T. Kuhn, L. Reggiani, and Y. Perlès, Solid-State Electron. **36**, 251 (1993).
[6] T. González, D. Pardo, L. Varani, and L. Reggiani, IEEE Trans. Electron Devices **ED-42**, 991 (1995).
[7] T. González, D. Pardo, L. Varani, and L. Reggiani, Appl. Phys. Lett. **63**, 3040 (1993).
[8] M. J. Martín, D. Pardo, and J. E. Velázquez, Appl. Phys. Lett. **71**, 3382 (1997).
[9] M. J. Martín, T. González, J. Velázquez, and D. Pardo, Semicond. Sci. Technol. **8**, 1291 (1993).
[10] M. J. Martín, D. Pardo, and J. E. Velázquez, J. Appl. Phys. **79**, 6975 (1996).
[11] M. J. Martín, D. Pardo, and J. E. Velázquez, J. Appl. Phys. **84**, 5012 (1998).
[12] R. People and J. C. Bean, Appl. Phys. Lett. **47**, 322 (1985).
[13] S. Tiwari, *Compound Semiconductor Device Physics* (Adademic, New York, 1992).
[14] K. Yeom, J. M. Hinckely, and J. Singh, Appl. Phys. Lett. **64**, 2985 (1994).
[15] M. V. Fischetti and S. E. Laux, J. Appl. Phys. **80**, 2234 (1996).
[16] L. E. Kay and T.-W. Tang, J. Appl. Phys. **70**, 1483 (1991).
[17] S. E. Laux and M. V. Fischetti, *Monte Carlo Device Simulation: Full Band and Beyond* (Kluwer, Boston, 1991).
[18] T. Gonzalez and D. Pardo, Solid-State Electron. **39**, 555 (1995).